Development 133, 319-329 doi:10.1242/dev.02210

The Vg1-related protein Gdf3 acts in a Nodal signaling pathway in the pre-gastrulation mouse embryo

Canhe Chen[1,*], Stephanie M. Ware[2,*], Akira Sato[3], Dianne E. Houston-Hawkins[4], Raymond Habas[3], Martin M. Matzuk[4,5,6], Michael M. Shen[1,†] and Chester W. Brown[4,7,†]

The formation of the anterior visceral endoderm (AVE) in the pre-gastrulation mouse embryo represents a crucial event in patterning of the anterior-posterior axis. Here, we show that the transforming growth factor β (Tgfβ) family member Gdf3 (growth-differentiation factor 3), a close relative of *Xenopus* Vg1, resembles the Tgfβ ligand Nodal in both its signaling activity and its role in AVE formation in vivo. Thus, in cell culture, Gdf3 signaling requires the EGF-CFC co-receptor Cripto and can be inhibited by Lefty antagonists. In *Xenopus* embryos, Gdf3 misexpression results in secondary axis formation, and induces morphogenetic elongation and mesendoderm formation in animal caps. In mouse embryos, *Gdf3* is expressed in the inner cell mass and epiblast, and null mutants frequently exhibit abnormal formation or positioning of the AVE. This phenotype correlates with defects in mesoderm and definitive endoderm formation, as well as abnormal *Nodal* expression levels. Our findings indicate that Gdf3 acts in a Nodal-like signaling pathway in pre-gastrulation development, and provide evidence for the functional conservation of Vg1 activity in mice.

KEY WORDS: Tgfβ signaling, EGF-CFC proteins, Anterior visceral endoderm, Mesendoderm formation

INTRODUCTION

A key event in formation of the anteroposterior axis of the mouse embryo is the induction of the anterior visceral endoderm (AVE), a specialized population of cells within the extra-embryonic visceral endoderm that overlies and patterns the adjacent epiblast (reviewed by Lu et al., 2001; Rossant and Tam, 2004). The AVE is formed in the most distal region of the post-implantation egg cylinder at 5.5 days post coitum (dpc), but then translocates to the prospective anterior side by 6.0 dpc (Rivera-Perez et al., 2003; Srinivas et al., 2004; Thomas et al., 1998), prior to the onset of gastrulation. Both formation as well as movement of the AVE require activity of the Nodal signaling pathway, whereas the AVE itself produces Nodal antagonists that are essential for patterning of the anterior epiblast (Brennan et al., 2001; Ding et al., 1998; Perea-Gomez et al., 2002; Yamamoto et al., 2004). As a consequence, anti-Nodal signals from the distal visceral endoderm become opposed to Nodal signals from the proximal epiblast, and together pattern the anteroposterior (AP) axis following movement of the AVE. The molecular regulation of AVE induction and Nodal signaling activities is therefore of central importance for AP axis patterning in the mammalian embryo.

However, despite many recent advances in understanding early embryo patterning, the function of one of the first Tgfβ superfamily members to be implicated in vertebrate development has remained poorly understood. The *Xenopus Vg1* gene was originally identified in a screen for vegetally localized maternal transcripts in the blastula stage embryo, and was proposed to act as an axial mesoderm inducer (Kessler and Melton, 1995; Melton, 1987; Thomsen and Melton, 1993; Weeks and Melton, 1987). Although subsequent analyses have identified *Vg1* orthologs in zebrafish (Dohrmann et al., 1996; Helde and Grunwald, 1993) and chick (Seleiro et al., 1996; Shah et al., 1997), no clear ortholog has been identified in mammalian genomes. An initial screen for *Vg1*-related genes in mice had isolated growth-differentiation factor 3 (*Gdf3*), which shares 79% amino acid similarity with Vg1 (Jones et al., 1992). Early phylogenetic comparisons had suggested that Gdf3 was most closely related to *Xenopus* Vg1 and mammalian Gdf1 (Burt and Law, 1994), but more recent analyses have grouped Gdf3 with members of the Bmp subfamily (e.g. Chang et al., 2002; Newfeld et al., 1999).

Several lines of evidence have suggested that Vg1 can signal through a pathway similar to that for Nodal, which plays crucial roles in AP patterning, formation of mesoderm, definitive endoderm and axial mesendoderm, and specification of the left-right axis (reviewed by Schier, 2003; Schier and Shen, 2000; Whitman, 2001). In particular, signaling by processed Vg1, like that of activin and Nodal, results in activation of Smad2, and can be antagonized by dominant-negative Smad2 mutants (Graff et al., 1996; Hoodless et al., 1999). In addition, the effects of Vg1 overexpression in *Xenopus* can be blocked by a dominant-negative form of Foxh1/FAST, a winged-helix transcription factor that mediates many key aspects of Nodal signaling (Watanabe and Whitman, 1999). Notably, recent work has shown that the effects of Vg1 and Gdf1 overexpression in zebrafish require the EGF-CFC protein Oep, and that mature Vg1 and Gdf1 proteins can interact with Oep as well as the mouse EGF-CFC protein Cripto (Tdgf1) (Cheng et al., 2003). This requirement for EGF-CFC proteins, which act as putative co-receptors for Nodal ligand (Gritsman et al., 1999; Reissmann et al., 2001; Yan et al., 2002; Yeo and Whitman, 2001), indicates that Vg1 and Gdf1 signal through a Nodal-like pathway.

[1]Center for Advanced Biotechnology and Medicine and Department of Pediatrics, University of Medicine and Dentistry of New Jersey-Robert Wood Johnson Medical School, Piscataway, NJ 08854, USA. [2]Department of Pediatrics, Cincinnati Children's Hospital Medical Center and University of Cincinnati College of Medicine, Cincinnati, OH 45229, USA. [3]Department of Biochemistry, University of Medicine and Dentistry of New Jersey-Robert Wood Johnson Medical School, Piscataway, NJ 08854, USA. [4]Department of Molecular and Human Genetics, Baylor College of Medicine, Houston, TX 77030, USA. [5]Department of Pathology, Baylor College of Medicine, Houston, TX 77030, USA. [6]Department of Molecular and Cellular Biology, Baylor College of Medicine, Houston, TX 77030, USA. [7]Department of Pediatrics, Baylor College of Medicine, Houston, TX 77030, USA.

*These authors contributed equally to this work
†Authors for correspondence (e-mail: mshen@cabm.rutgers.edu; cbrown@bcm.tmc.edu)

Accepted 11 November 2005

Owing to the similar activities of Vg1 and Nodal, it has remained unclear whether there is a conservation of Vg1-related activities during mammalian development, or indeed whether endogenous Vg1 has essential functions. To address these issues, we have investigated the potential conservation of Vg1 function through analyses of mouse *Gdf3*. We find that Gdf3 has activity in a cell culture assay for Nodal signaling, can form a complex with activin receptors and the EGF-CFC protein Cripto, and has activities similar to that of Nodal in *Xenopus* embryos and animal caps. We show that *Gdf3* is expressed in pre-implantation and early post-implantation mouse embryos, and that ~35% of null mutants display pre-gastrulation and gastrulation defects consistent with the absence or mispositioning of the AVE, with the remainder surviving to adulthood. Our results suggest that Gdf3 has a crucial Nodal-like activity and is likely to represent a functional homolog for Vg1 in early mouse development.

MATERIALS AND METHODS

Cell culture assay for Gdf3 activity

The mouse *pcDNA3-bf-Gdf3* and *pcDNA3-bv-Gdf3* expression constructs were generated by PCR from a mouse Gdf3 cDNA template (McPherron and Lee, 1993), and contain a heterologous *Xenopus* Bmp2 prodomain and a FLAG or V5 epitope-tag inserted immediately after the proprotein convertase cleavage site (Fig. 1A). Luciferase assays for Gdf3 and Nodal activities were performed as described (Yan et al., 2002). Co-transfection of an expression construct for β-galactosidase was used to normalize for transfection efficiency, and addition of empty *pcDNA3* vector was used to maintain constant amounts of transfected DNA. Protein expression was detected by western blotting using a goat anti-mouse Gdf3 polyclonal antiserum (R&D Systems), polyclonal antiserum against mouse Nodal (Yan et al., 2002), polyclonal antiserum against mouse Lefty1 (Chen and Shen, 2004), or a monoclonal anti-FLAG M2 antibody (Sigma).

Protein cross-linking and co-immunoprecipitation analysis

Reversible chemical crosslinking with 0.5 mM DTSSP [3,3′-dithiobis(sulfosuccinimidyl proprionate)] (Pierce) and co-immunoprecipitation were carried out as described previously (Chen and Shen, 2004). To detect the association of Gdf3 and Lefty1 in conditioned media, 293T cells were transfected with *pcDNA3-bf-Gdf3* and *pcDNA3-Lefty1*; culture supernatants were collected 48 hours post-transfection and directly subjected to immunoprecipitation with anti-FLAG M2 antibody (Sigma). For all other experiments, crosslinking with DTSSP was carried out prior to co-immunoprecipitation, using whole-cell lysates prepared with RIPA114 buffer (Yan et al., 2002). The kinase-inactive receptor mutants ActRIIB(K217R)-Myc and ActRIB(K234R)-HA have been described previously (Yeo and Whitman, 2001). Western blotting was performed using the antibodies described above, as well as monoclonal anti-HA antibody (Covance) and anti-Myc antibody (Santa Cruz).

Xenopus microinjection and animal cap assays

Ovulation, in vitro fertilization, and embryo and explant cultures were carried out as described (Habas et al., 2001; Kato et al., 2002). Sequences corresponding to mouse Gdf3, bf-Gdf3 and Nodal were cloned into the pCS2+ vector for in vitro transcription using a mMachine SP6 system (Ambion). Capped mRNA was injected into the two ventral marginal zones of the four-cell embryo for phenotypic assays or into the animal hemisphere of *Xenopus* embryos at the two-cell stage. Animal caps were explanted at blastula stages 8.5-9 and cultured to early gastrula stage 11 for total RNA extraction and RT-PCR analysis. For phenotypic assays, embryos were raised to stage 30 in 0.1×MMR.

Gene targeting and phenotypic analysis

Gene targeting was performed as described (Bradley, 1987; Matzuk et al., 1992), using a 129S6SvEv-derived ES cell line derived from AB2.1. Sixty-two percent of clones resistant to both HAT and FIAU (n=52) were correctly targeted, as determined by Southern blot analysis using both 5′ and 3′ probes. Four independent clones were injected into mouse blastocysts, giving rise to germline male chimeras that sired mutant mice with identical phenotypes.

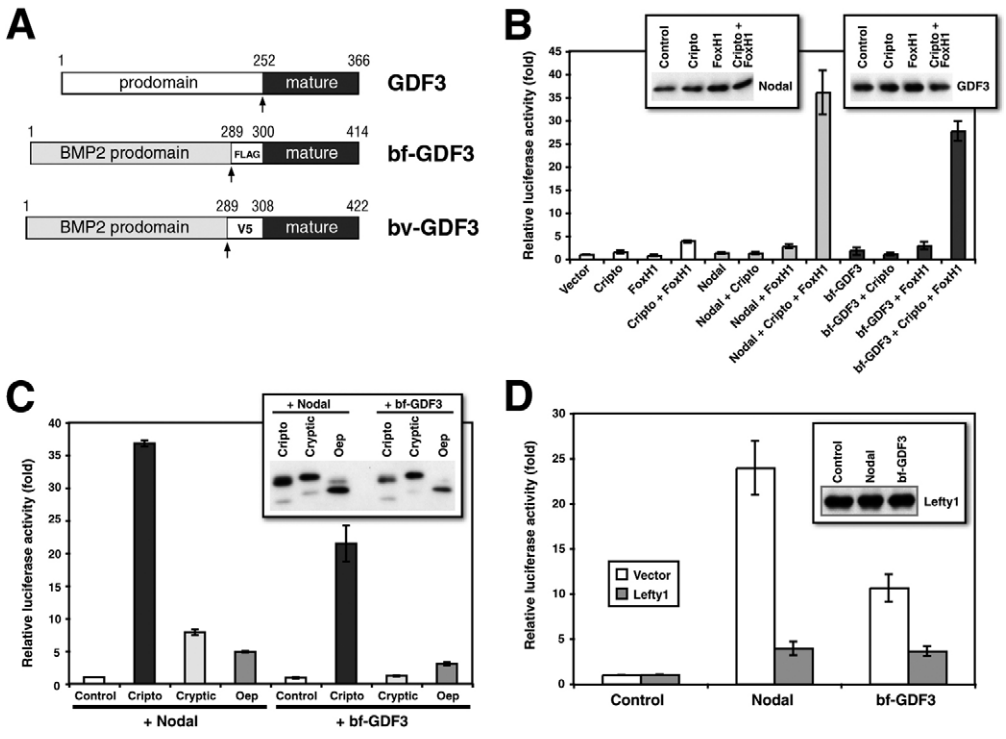

Fig. 1. Comparison of Gdf3 and Nodal signaling activities. (**A**) Schematic depiction of mouse Gdf3 and modified Gdf3 proteins; the sites of prodomain cleavage is indicated (arrows). (**B**) Gdf3 activity is Cripto and Foxh1 dependent. The indicated plasmids were co-transfected into 293T cells together with the *A3-luc* reporter. (Insets) Western blot detection of mature Nodal (~12 kDa) and mature Gdf3 (~17 kDa) proteins in conditioned media using α-Nodal antibody or α-Gdf3 antibody. (**C**) Gdf3 activity is facilitated by Cripto, but not Cryptic. 293T cells were co-transfected with expression vectors for Nodal or bf-Gdf3, Foxh1 and FLAG-epitope-tagged Cryptic, Cripto or Oep; control samples correspond to cells transfected with Nodal or bf-Gdf3 and Foxh1 without EGF-CFC proteins. (Inset) Western blot detection of EGF-CFC proteins in cell lysates using α-FLAG antibody (FLAG-Cryptic, ~22 and ~20 kDa; FLAG-Cripto, ~21 and ~19 kDa; FLAG-Oep, ~21 kDa). (**D**) Lefty1 inhibits Gdf3 activity. Cells were co-transfected with expression constructs for Nodal or bf-Gdf3, Cripto and Foxh1, in the presence or absence of Lefty1; controls correspond to these cells without Nodal or bf-Gdf3 transfection. (Inset) Western blot detection of mature Lefty1 protein (~30 kDa) in conditioned media. In all panels, assays were performed in triplicate; error bars represent s.d.

Whole-mount in situ hybridization was carried out as described (Ding et al., 1998; Wilkinson, 1992), using probes labeled by the DIG RNA Labeling Kit (Boehringer Mannheim). Most of the marker analysis was performed using a C57BL/6J congenic strain, although similar data were obtained using a C57BL/6J-129S6/SvEv mixed genetic background. Histological analysis was performed on formalin-fixed paraffin sections of whole decidua stained with Hematoxylin and Eosin.

Real-time RT-PCR analysis

Total RNA from individual embryos in the C57BL/6 strain background was isolated using the RNeasy Micro Kit (Qiagen) and reverse-transcribed to generate first-strand cDNA (Invitrogen). Real-time PCR amplification was performed using a Mx4000 quantitative PCR instrument with SYBR Green QPCR Master Mix (Stratagene). The primer pairs used were: for *Nodal*, 5′ CCA TGC CTA CAT CCA GAG CCT GC 3′ and 5′ TGG TGT TCC AGG AGG ACC CTG CC 3′; for *Gdf1*, 5′ TTC TGC CAG GGC ACG TGC G 3′ and 5′ GGA GCA GCT GCG TGC ATG AG 3′; and for *Gapdh*, 5′ TGC GAC TTC AAC AGC AAC TC 3′ and 5′ GCC TCT CTT GCT CAG TGT CC 3′. Three independent reverse-transcription reactions were performed on each total RNA, followed by real-time PCR amplification in triplicate and normalization against *Gapdh* levels.

RESULTS

Gdf3 activity in a Nodal-like signaling pathway

To investigate the properties of Gdf3, we examined whether Gdf3 protein can be expressed and signal in a Nodal-like pathway in mammalian cell culture. When we transfected a native Gdf3 expression construct into 293T human embryonic kidney cells, we observed that this native construct was processed poorly, with very low levels of mature ligand detected in conditioned media (Fig. 1A; see Fig. S1A in the supplementary material). To circumvent the inefficient processing of native Gdf3, we replaced the Gdf3 prodomain with that of *Xenopus* Bmp2, which is processed efficiently in 293T cells (Chen and Shen, 2004), and added a FLAG or V5 epitope tag at the N terminus of the mature ligand for ease of protein detection (Fig. 1A). The resulting bf-Gdf3 (Bmp2 prodomain-FLAG-mature Gdf3) fusion protein is expressed and processed efficiently in conditioned media of transfected 293T cells (see Fig. S1A in the supplementary material). We noted that there were several Gdf3 proprotein and mature species detected by western blotting; consensus glycosylation sequences located in the mature Gdf3 sequence and in the Gdf3 and Bmp2 prodomains suggest that these species differ in their levels of N-glycosylation.

Given the body of evidence that Vg1 signals in a pathway similar to that of Nodal, we examined the activity of these Gdf3 protein products using a luciferase reporter assay that we developed for Nodal activity in transfected 293T cells (Yan et al., 2002). This assay relies upon reconstitution of the essential signaling components Cripto and Foxh1, which are not expressed in 293T cells [nor are Nodal, Gdf1, Gdf3, Lefty1 or Lefty2 (Chen and Shen, 2004; Yan et al., 2002) (C.C. and M.M.S., unpublished)]; moreover, Bmp4 does not display activity in this assay (Yan et al., 2002). When Nodal is co-transfected with Cripto and Foxh1 into 293T cells, signaling activity can be detected using the activin/Nodal-responsive luciferase reporter *A3-luc* (Fig. 1B). When co-expressed with Cripto and Foxh1, native Gdf3 gives a low but detectable level of activity, consistent with the low levels of mature ligand detected in conditioned media, whereas the modified bf-Gdf3 results in significant signaling activity (Fig. 1B; see Fig. S1 in the supplementary material).

As Gdf3 and Nodal displayed similar activities in this cell culture assay, we examined whether these ligands would behave identically if parameters of this assay were altered. As is the case for Nodal (Yan et al., 2002), we found that Gdf3 activity was absolutely dependent upon expression of EGF-CFC proteins and Foxh1 (Fig. 1B). We further explored the EGF-CFC dependence of Gdf3 by examining whether other EGF-CFC proteins could mediate Gdf3 signaling, and observed that Gdf3 displayed less activity in combination with mouse Cryptic (Cfc1) or fish Oep than with mouse Cripto (Fig. 1C). Finally, we found that co-expression of Lefty1 or Lefty2 could inhibit Gdf3 signaling activity (Fig. 1D; data not shown), analogous to Nodal (Chen and Shen, 2004). Taken together, these results indicate that Gdf3 can use a signaling pathway highly similar to that for Nodal.

Interaction of Gdf3 and Cripto in a receptor complex

To address whether Gdf3 signaling is mediated by activin receptors, and examine the formation of a Gdf3 receptor complex, we used reversible protein crosslinking/co-immunoprecipitation. We co-expressed epitope-tagged type I (ActRIB/ALK4) and type II (ActRIIB) receptors together with bf-Gdf3 and FLAG-tagged Cripto (f-Cripto) in 293T cells, and examined the proteins immunoprecipitated together with ActRIIB following crosslinking with the membrane-impermeable agent DTSSP (Chen and Shen, 2004).

Interestingly, we found that bf-Gdf3 proprotein interacted equally well with activin receptors in the absence or presence of Cripto, similar to our previous observations with Nodal (Fig. 2A) (Chen and Shen, 2004). However, the interaction of mature Gdf3 ligand with activin receptors was greatly enhanced in the presence of Cripto, similar to previous observations of EGF-CFC dependent receptor complex formation with mature Nodal in frog animal caps (Fig. 2A, compare lanes 4 and 6) (Cheng et al., 2003; Yeo and Whitman, 2001). We also obtained similar results with native Gdf3 in this assay, although the levels of mature ligand present in activin receptor complexes were low (data not shown), indicating that our findings are not a consequence of the use of a heterologous Bmp2 prodomain. Furthermore, in crosslinking/co-immunoprecipitation experiments in the absence of co-transfected activin receptors, we found that Cripto interacted equally well with the bv-Gdf3 proprotein (Bmp2 prodomain-V5-mature Gdf3) as with the mature ligand (Fig. 2B). In combination, these findings indicate that Cripto specifically enhances and/or stabilizes receptor complex formation by mature Gdf3 ligand with activin receptors.

Finally, we investigated the basis by which Lefty1 can inhibit Gdf3 signaling activity (Fig. 2C). We and others have shown that Lefty proteins can inhibit Nodal signaling through an interaction with EGF-CFC proteins (Chen and Shen, 2004; Cheng et al., 2004), as well as with mature Nodal ligand in conditioned media (Chen and Shen, 2004). Consequently, we examined whether Lefty1 could interact with Gdf3 in conditioned media in the absence of crosslinking. We found that Gdf3 could specifically immunoprecipitate the mature Lefty1 protein, but not the Lefty1 proprotein (Fig. 2C), similar to our previous findings with Nodal (Chen and Shen, 2004).

Similar effects of *Gdf3* and *Nodal* misexpression in *Xenopus* embryos

To examine whether Gdf3 signals in a Nodal-like pathway in vivo, we performed gain-of-function assays in *Xenopus laevis* embryos to compare the effects of *Gdf3* and *Nodal* misexpression. Previous studies have shown that misexpression of mouse *Nodal* in the ventral marginal zone can dorsoanteriorize *Xenopus* embryos, and induce dose-dependent expression of dorsal mesoderm markers in animal caps (Jones et al., 1995; Joseph and Melton, 1997; Takahashi et al., 2000). Following microinjection of mRNAs into the two ventral

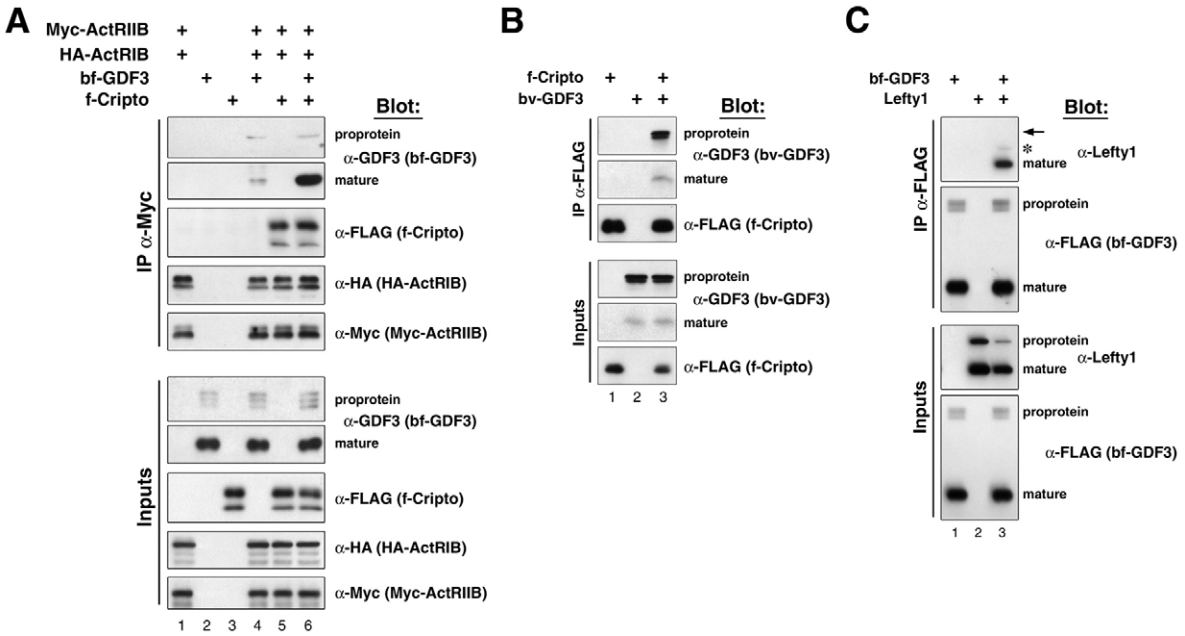

Fig. 2. Interactions of Gdf3 with activin receptors, Cripto and Lefty1. (**A**) Formation of a Gdf3 receptor complex. 293T cells were transfected with the indicated expression constructs, followed by crosslinking with the membrane-impermeable reagent DTSSP, immunoprecipitation of Myc-tagged ActRIIB from cell lysates and reversal of crosslinking; kinase-inactive activin receptor mutants were used in order to decrease receptor internalization. Western blots of immunoprecipitated and input proteins are shown, detected using the following antibodies: α-Gdf3 (bf-Gdf3 proprotein, ~49 kDa; mature bf-Gdf3, ~17 kDa); α-FLAG (f-Cripto, ~21 kDa); α-HA (ActRIB-HA, ~54 kDa); α-Myc (ActRIIB-6xMyc, ~75 kDa). (**B**) Cripto interacts with Gdf3. Expression constructs were co-transfected into 293T cells, followed by crosslinking with DTSSP, immunoprecipitation of FLAG-tagged Cripto (f-Cripto) from cell lysates and reversal of crosslinking. Western blots are shown using the following antibodies: α-V5 (bv-Gdf3 proprotein, ~50 kDa) and α-FLAG (f-Cripto, ~21 kDa). (**C**) Gdf3 interacts with Lefty1 in conditioned media in the absence of crosslinking. The mature form of Lefty1 is preferentially immunoprecipitated; the expected positions of the Lefty1 proprotein (arrow) and a mature Lefty1 variant generated by use of an alternative prodomain cleavage site (asterisk) are indicated. Proteins were detected by western blotting using the following antibodies: α-FLAG (bf-Gdf3 proprotein, ~49 kDa; mature bf-Gdf3, ~17 kDa) and α-Lefty1 (Lefty1 proprotein, ~40 kDa; mature Lefty1, ~30 kDa).

marginal zones of four-cell stage embryos, we observed the formation of partial secondary axes in response to low levels of Nodal (10 pg) and higher levels of Gdf3 or bf-Gdf3 (100 pg and 50 pg, respectively) (Fig. 3A-D; Table 1). Similarly, expression of low doses of Nodal (50 pg) or bf-Gdf3 (50 pg) in animal caps induced morphogenetic elongation (79%, *n*=33 for Nodal; 39%, *n*=31 for bf-Gdf3), and expression of markers of early pan-mesoderm [*Xbra* (brachyury)], dorsal mesoderm [*Xwnt8*, chordin, *Gsc* (goosecoid)] and endoderm (*Mixer*), but not the dorsal marker *Xnr3* (Fig. 3E-I). We also observed morphogenetic elongation with high doses of native Gdf3 (500 pg) (76%, *n*=33), as well as induction of *Xbra* and *Mixer* (1000 pg), suggesting that unmodified Gdf3 is poorly processed in *Xenopus* embryos, but possesses similar activity to bf-Gdf3 (Fig. 3I).

Restricted expression of *Gdf3* in inner cell mass and epiblast

To gain insight into potential roles for *Gdf3* in vivo, we assessed its expression pattern in wild-type mouse embryos at pre-implantation and early post-implantation stages. We found that *Gdf3* expression initiates in a population of inner cells at the morula stage (Fig. 4A), with no expression detected at earlier pre-implantation stages (data not shown). Subsequently, *Gdf3* expression is limited to the inner cell mass at the blastocyst stage (Fig. 4B), consistent with its conserved expression in mouse and human ES cells (Sato et al., 2003). During post-implantation development, *Gdf3* expression occurs uniformly throughout the epiblast at 5.5 and 6.0 dpc, but is not detectable in the extra-embryonic ectoderm or visceral endoderm (Fig. 4C-F). Notably, *Gdf3* expression appears to cease by 6.5 dpc, prior to the onset of gastrulation, with no further expression detected by in situ hybridization during gastrulation or through 9.5 dpc, including in primordial germ cells. Thus, *Gdf3* expression is highly restricted to the pluripotent cells of the inner cell mass and epiblast.

Early embryonic lethality in a subset of *Gdf3* homozygous null mutants

To investigate the biological functions of *Gdf3*, we produced mice with a null mutation at the *Gdf3* locus (see Fig. S2 in the supplementary material). Although we could readily recover fertile and healthy *Gdf3*$^{-/-}$ homozygous mice, we observed these were significantly under-represented among progeny from heterozygote intercrosses (data not shown). Consequently, we examined the phenotypes of *Gdf3* mutants at embryonic stages, and found that ~35% (*n*=127) of *Gdf3* homozygotes displayed abnormal phenotypes at 6.0 to 8.5 dpc (Table 2). The most severely affected embryos were either resorbing (5%), or corresponded to empty visceral yolk sacs at 8.5 dpc (11%) (Fig. 5A). Less severely affected embryos exhibited characteristic morphological phenotypes, including prominent constriction at the embryonic/extra-embryonic junction, poorly differentiated anterior structures and abnormal mesoderm derivatives (21%) (Fig. 5B-G). Similar frequencies of embryonic lethality, as well as embryonic phenotypes were observed in *Gdf3*$^{-/-}$ 129SvEv inbred and C57BL/6J congenic mice that had been backcrossed for seven generations (Table 2; data not shown), suggesting that the phenotypic heterogeneity is not strongly

influenced by strain background. Phenotypic analysis of embryos from homozygous by heterozygous crosses excluded the possibility of a *Gdf3* maternal effect (C.C. and M.M.S., unpublished).

Defects in AVE and primitive streak derivatives in *Gdf3* mutants

To analyze the phenotypic abnormalities observed in *Gdf3* mutants, we performed whole-mount in situ hybridization using tissue-specific markers at gastrulation and pre-gastrulation stages. Initially, we examined the expression of early mesoderm markers, such as *Foxa2* (Hnf3β), which is expressed in the anterior primitive streak and subsequently in the node and axial mesendoderm, but is greatly diminished or absent in 50% (*n*=6) of *Gdf3* homozygotes at 6.75 dpc (Fig. 6A,B). We also found that expression of *Lhx1* (*Lim1*) in lateral mesoderm emerging from the primitive streak was reduced or absent in 50% (*n*=4) of *Gdf3* homozygotes at 6.75 dpc (Fig. 6C,D), and in 64% (*n*=11) of *Gdf3* homozygotes at 7.5 dpc (data not shown). Similar defects in nascent mesoderm formation were observed using the markers *Wnt3* and *Fgf8* (data not shown). By contrast, early neural specification and patterning appeared to be normal, as *Otx2* expression in prospective forebrain and midbrain regions was unaffected in *Gdf3* homozygotes (*n*=15) at 7.0-7.5 dpc (Fig. 6E,F). However, this early expression was often not maintained, as shown by the severely decreased or absent expression of *Otx2* in 63% (*n*=8) of *Gdf3* mutants at 8.5 dpc (data not shown).

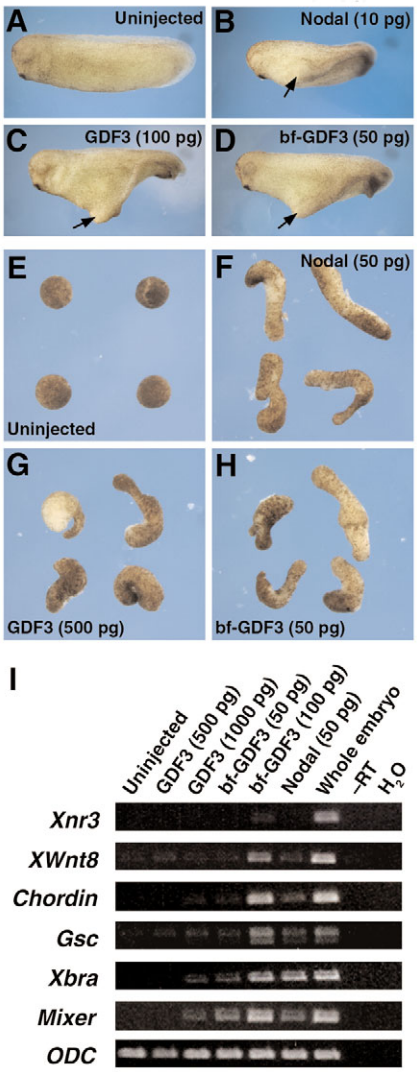

Fig. 3. Gdf3 induces secondary axis and mesendoderm formation in *Xenopus* embryos. (**A-D**) Secondary axis formation following ventral marginal zone injection. Morphology of control uninjected embryo (A) and embryos injected with the indicated doses of Nodal (B), Gdf3 (C) or bf-Gdf3 (D) mRNAs; arrows indicate secondary axis formation. (**E-H**) Gdf3 induces morphogenetic elongation in animal cap explants. Unlike control uninjected caps (E), animal caps injected with the indicated doses of Nodal (F), Gdf3 (G) or bf-Gdf3 (H) mRNAs undergo morphogenetic elongation, as scored at stage 20. (**I**) Mesendoderm formation in animal cap assays. High doses of Gdf3 (500-1000 pg) result in weak induction of *Xbra* and *Mixer*, while low doses of Nodal (50 pg) and bf-Gdf3 (50-100 pg) result in strong induction of markers for mesoderm (*Xbra*, *Gsc*, chordin and *Xwnt8*) and endoderm (*Mixer*), but not the dorsal marker *Xnr3*. Ornithine decarboxylase (*Odc*) is used as an internal control. –RT, no reverse transcriptase added.

Further analyses demonstrated severe defects in AVE formation and movement as well as loss of definitive endoderm in a subset of *Gdf3* homozygotes. Using the marker *Cerl* (cerberus-like), we observed that definitive endoderm formation was greatly reduced or absent in 60% of (*n*=5) *Gdf3* homozygotes at 7.0 dpc (Fig. 6G,H). Additional analyses showed that *Gdf3* homozygotes had defects in expression of *Hesx1* at 6.75 dpc (38%, *n*=8) and *Hex* at 6.5-7.0 dpc in the AVE (31%, *n*=13) (Fig. 6I-M); similar results were observed for *Lhx1*, which is also expressed in the AVE (Fig. 6C,D; data not shown). Notably, these analyses identified *Gdf3* homozygotes with reduction or absence of the AVE (19%, *n*=26) (Fig. 6D,J,L), or mislocalization of the AVE in the distal visceral endoderm (8%, *n*=26) (Fig. 6M), suggesting a failure in AVE movement to the prospective anterior side.

Examination of less severely affected *Gdf3* mutants failed to reveal additional defects in body patterning at later stages of development, including left-right axis specification (Fig. 6N,O; data not shown). In particular, morphologically normal *Gdf3* homozygotes displayed correct left-sided *Nodal* expression in the lateral plate mesoderm at 8.0 dpc (67% four- to eight-somite stage embryos, *n*=9) (Fig. 6N); a few morphologically abnormal *Gdf3* embryos lacked left-sided *Nodal* expression (Fig. 6O), but this was probably due to absence of the lateral plate mesoderm.

Surprisingly, our marker analyses also revealed an unusual subset of *Gdf3* homozygotes that display a partial axis duplication. Although *Gdf3* homozygotes frequently displayed reduced or absent expression of *T* (brachyury), which is normally found in the node and axial mesoderm at 8.0 dpc (Fig. 6P,Q), rare homozygous embryos (5%, *n*=57) showed twinned axial mesoderm staining, corresponding to duplicated notochords in sections (Fig. 6R,S) and indicating that secondary axis formation is an infrequent consequence of *Gdf3* inactivation.

Altered expression of *Nodal* in *Gdf3* mutant embryos

Overall, the phenotypic abnormalities observed in affected *Gdf3* mutants strongly resemble those observed in mutants for several genes in the Nodal signaling pathway (see Discussion). To assess potential effects on this pathway, we examined expression of *Nodal* itself in *Gdf3* homozygotes at 6.0-6.75 dpc. In wild-type embryos prior to gastrulation, *Nodal* displays graded expression in the epiblast, with highest levels in the posterior and proximal region (Fig. 6T,Z). Interestingly, we found that 2/15 (13%) *Gdf3* homozygotes showed apparent downregulation of *Nodal* expression at 6.0 dpc, with limited staining in the proximoposterior epiblast (Fig. 6U), whereas 3/15 (20%) *Gdf3* mutants showed strong

Table 1. Phenotypes resulting from ventral marginal zone injections in *Xenopus* embryos

	Number	Partial secondary axis	Posterior defect*	Normal
Uninjected	90	0/90 (0%)	0/90 (0%)	90/90 (100%)
GDF3 (100 pg)	76	40/76 (53%)	33/76 (43%)	3/76 (4%)
bf-GDF3 (50 pg)	65	36/65 (55%)	28/65 (43%)	1/65 (2%)
Nodal (10 pg)	72	12/72 (17%)	60/72 (83%)	0/72 (0%)

*Embryos with posterior defects had abnormal blastopore closure, resulting in an open neural tube in the posterior; in addition, many embryos contained a small darkly pigmented protrusion in the posterior region that could not be classified as a partial axis.

upregulation of *Nodal* expression throughout the epiblast (Fig. 6V,A′). Similarly, quantitative real-time RT-PCR analysis of individual embryos at 6.0 dpc revealed significant downregulation of *Nodal* expression in 5/26 *Gdf3* homozygotes relative to wild-type controls, while 3/26 *Gdf3* homozygotes displayed significant *Nodal* upregulation (see Fig. S3A in the supplementary material). Notably, the percentage of embryos showing altered levels of *Nodal* expression by real-time PCR (34%, *n*=73) (analysis of 26 embryos is shown in Fig. S3A in the supplementary material; data for an additional 47 are not shown), is similar to the percentage displaying AVE defects by marker analyses (27%, *n*=26), as well as to the percentage with morphological defects at 6.75 and 7.5 dpc (29% and 35%, respectively; Table 2). This correlation suggests that the *Gdf3* homozygotes with AVE defects also display altered *Nodal* expression at 6.0 dpc and undergo abnormal development, while the remaining *Gdf3* homozygotes are phenotypically wild type.

At later stages, we also observed considerable variation in the *Nodal* expression patterns and morphologies of *Gdf3* homozygotes. In wild-type embryos at early and mid-streak stages, *Nodal* expression persists in the posterior epiblast and is downregulated in the primitive streak, but is slightly upregulated in the posterior visceral endoderm overlying the streak (Fig. 6W,B′). We found that a significant number of *Gdf3* homozygotes (44%, *n*=9) showed abnormal morphology and *Nodal* expression at 6.75 dpc. We observed more intense posterior *Nodal* expression in one out of nine *Gdf3* homozygotes, which showed a greatly expanded primitive streak in sections (Fig. 6X,C′); such embryos may give rise to the axis duplications observed at later stages (Fig. 6R,S). Furthermore, two out of nine (22%) homozygous mutants displayed a ‘conical’ morphology that was associated with a radially symmetric shape in cross-section (Fig. 6Y,D′). Strikingly, these embryos were filled with cells of mesodermal appearance and displayed circumferential upregulation of *Nodal* expression in the visceral endoderm, suggesting that most of the epiblast had undergone streak formation and become mesoderm.

Additional marker analyses were consistent with the interpretation that *Gdf3* mutants have primary defects in AVE formation and movement, with consequent effects on expression of *Nodal*. Examination of *Cripto* expression at 6.75 dpc showed that most *Gdf3* homozygotes showed normal expression in the posterior epiblast, with the exception of the unusual ‘conical’ mutants, which showed strong upregulation throughout the epiblast (Fig. 6E′,F′; data not shown). The expression patterns of *Lefty1* in the AVE at 6.0 dpc and *Lefty2* in nascent mesoderm at 6.75 dpc were similar to that described above for other AVE and mesodermal markers, respectively (data not shown). Furthermore, expression of *Bmp4* in the extra-embryonic ectoderm is dependent upon Nodal signaling in the adjacent proximal epiblast (Brennan et al., 2001), but no effects on *Bmp4* expression were observed in *Gdf3* mutants at 6.5 dpc (*n*=7) (Fig. 6G′,H′), suggesting that Nodal activity in the proximal epiblast remains at least partially intact. Finally, as Gdf1 can also signal through a Nodal-like pathway, we examined the expression of *Gdf1*, which is expressed at low levels throughout the epiblast at 5.5 dpc and becomes upregulated at ~5.75 dpc (Wall et al., 2000) (this

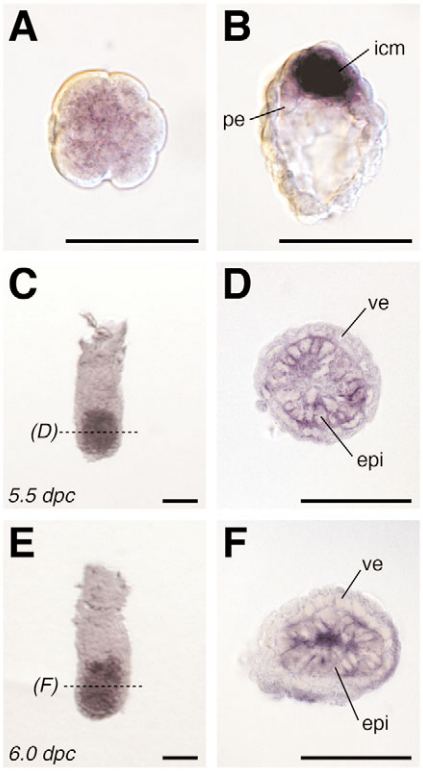

Fig. 4. *Gdf3* expression in pre-implantation and early post-implantation mouse embryos. (**A**,**B**) Expression of *Gdf3* is found at low levels in the inner cells of compacted morula at the 16-cell stage (A), and is later expressed at higher levels in the inner cell mass (icm) at the blastocyst stage (B), with no expression in the trophoblast or primitive endoderm (pe). (**C**-**F**) After implantation, expression is restricted to the embryonic epiblast (epi) at 5.5 dpc (C,D) and 6.0 dpc (E,F), and is not found in the visceral endoderm (ve) or extra-embryonic ectoderm; expression disappears prior to primitive streak formation. Scale bars: 50 μm.

Table 2. Frequency of embryonic phenotypes in *Gdf3*$^{-/-}$ embryos

	6.0 dpc	6.75 dpc	7.5 dpc	8.5 dpc
Abnormal	20	31	40	27
Empty yolk sac/resorbed	0	3	11	20
Total	117	119	144	127
Ratio	17%	29%	35%	37%

Mice were in a C57BL/6J congenic background for the 6.0, 6.75 and 7.5 dpc analyses, and in a C57BL/6J-129S6/SvEv mixed genetic background for the 8.5 dpc analysis.

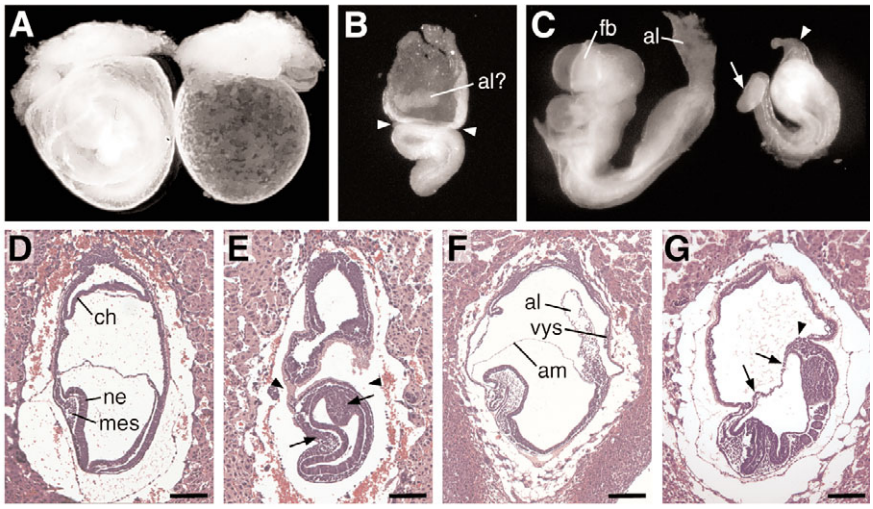

Fig. 5. Morphology and histology of *Gdf3* mutant embryos. (**A**) Two *Gdf3*$^{-/-}$ embryos at 8.5 dpc, showing a phenotypically wild-type embryo (left) and a severe mutant that consists of an empty visceral yolk sac (right). (**B**) A *Gdf3*$^{-/-}$ mutant at 8.5 dpc displays an abnormal embryonic region and prominent constriction at the embryonic/extra-embryonic boundary (arrowheads); an allantois-like structure (al?) is present. (**C**) Two *Gdf3*$^{-/-}$ embryos at 8.0 dpc, with a phenotypically wild-type embryo (left) and an abnormal embryo (right) with reduced anterior structures (arrow) and an ectopic projection (arrowhead). (**D-G**) Hematoxylin-Eosin staining of paraffin wax-embedded sections through decidua containing *Gdf3*$^{-/-}$ embryos at 7.5 dpc (D,E) and 8.0 dpc (F,G). In comparison with the phenotypically wild-type embryos (D,F), the severely affected mutant in E shows an embryonic/extra-embryonic boundary constriction (arrowheads) and an abnormal embryonic region containing mesoderm (arrows). The less-affected embryo in G lacks an allantois (arrowhead) and has visceral yolk sac-like tissue in place of an amnion (arrows). Scale bars: 200 μm. Abbreviations: al, allantois; am, amnion; ch, chorion; fb, forebrain; mes, mesoderm; ne, neuroectoderm; vys, visceral yolk sac.

work). We observed a similar expression pattern and temporal onset of *Gdf1* upregulation in *Gdf3* homozygotes (n=22) and wild-type controls (n=17) at 5.5-6.0 dpc (Fig. 6I′,J′; data not shown). In addition, quantitative real-time PCR analysis confirmed similar levels of *Gdf1* expression in individual wild-type and *Gdf3* mutant embryos at 6.0 dpc (see Fig. S3B in the supplementary material).

DISCUSSION

Our combined biochemical and molecular genetic analyses of Gdf3 function have provided strong evidence for its Nodal-like activity. The characteristic features of the *Gdf3* null phenotype imply that Gdf3 represents an important component of Nodal pathway activity at pre-gastrulation stages. Moreover, our findings uncover conserved functions of *Vg1*-related genes in vertebrate development, and raise the possibility that Nodal pathway activity may play an earlier role in mouse embryogenesis than hitherto appreciated.

Gdf3 functions in a Nodal-related pathway

Our studies provide three principal lines of evidence that Gdf3 acts in a Nodal-related pathway. First, we have shown that Gdf3 signaling in cell culture displays the defining features of the Nodal pathway in its requirement for EGF-CFC proteins and ability to be inhibited by Lefty proteins. At the biochemical level, Gdf3 can form complexes with activin receptors, and interacts with both Cripto and Lefty proteins in a manner highly reminiscent of Nodal. Second, we have demonstrated that misexpression of bf-Gdf3 and Nodal in *Xenopus* embryos and animal caps results in essentially indistinguishable phenotypes. In particular, the ability of bf-Gdf3 to induce dorsal mesoderm markers in animal caps underscores the similarity of Gdf3 and Nodal activities, and suggests that Gdf3 activity is specific for a Nodal-like pathway in vivo. Finally, the majority of affected *Gdf3* mutants display phenotypes associated with loss- or reduction-of-function for components of the Nodal signaling pathway. In particular, Nodal signaling from the epiblast is essential for AVE formation (Brennan et al., 2001; Norris et al., 2002), as well as its movement from its original distal position to the prospective anterior side (Ding et al., 1998; Lowe et al., 2001; Yamamoto et al., 2004). Failure to form the AVE leads to the absence of anterior structures and is often correlated with an empty yolk sac phenotype (Brennan et al., 2001; Waldrip et al., 1998), similar to that observed in the most severely affected *Gdf3* mutants. Less severely affected *Gdf3* mutant embryos exhibit defects in mesoderm and definitive endoderm formation, similar to *Nodal* null and hypomorphic mutants (Conlon et al., 1994; Lowe et al., 2001; Norris et al., 2002; Zhou et al., 1993). In addition, *Gdf3* mutants display reduced anterior structures, most probably owing to loss of axial mesendoderm, which is commonly observed in mutants for Nodal pathway components (Dunn et al., 2004; Hoodless et al., 2001; Lowe et al., 2001; Song et al., 1999; Vincent et al., 2003; Yamamoto et al., 2001).

Based on our findings, we propose that Gdf3 functions through a Nodal-like pathway to provide a crucial signal for AVE formation and movement in pre-gastrulation development (Fig. 7A). The variability of the *Gdf3*-null phenotype might thus be due to stochastic differences in the ability of *Nodal* to provide sufficient pathway activity to compensate for the absence of *Gdf3*. *Gdf3* may also be required subsequently for mesoderm and definitive endoderm formation; however, as *Nodal* expression is perturbed in the absence of *Gdf3,* we are unable to distinguish whether the gastrulation phenotypes of *Gdf3* mutants represent primary or secondary consequences of *Gdf3* inactivation. A second, non-mutually exclusive possibility is that Gdf3 may act to upregulate *Nodal* expression itself, through its potential to activate the Nodal positive autoregulatory loop. This model is perhaps less plausible as deletion of the *Nodal* autoregulatory enhancer results in a relatively mild left-right patterning defect (Norris et al., 2002); however, the recent elucidation of a second Nodal-responsive enhancer raises the possibility that autoregulation may play an important role at earlier stages of development (Saijoh et al., 2005).

Unexpectedly, we have observed that *Nodal* expression can either be downregulated or upregulated in the absence of *Gdf3*. These apparently opposite outcomes can potentially be explained by the requirement of *Gdf3* for AVE induction and movement. In the absence of *Gdf3,* the AVE may be able to form, but be unable to move, leading to retention of *Nodal* expression in the proximal epiblast, resulting in reduction or absence of mesoderm and definitive endoderm formation (Fig. 7B). However, if the AVE fails to form, *Nodal* expression would remain at high levels throughout the epiblast (Fig. 7B), similar to the phenotype of

Smad2-null mutants (Brennan et al., 2001; Waldrip et al., 1998). In addition, overexpression of *Nodal* might lead to expansion and splitting of the primitive streak at early gastrulation stages, as well as partial axis duplications, as expression of Nodal pathway inhibitors in the AVE is necessary to suppress formation of a secondary axis (Bertocchini and Stern, 2002; Perea-Gomez et al., 2002). Similar phenotypes have been observed in other cases of Nodal pathway upregulation, such as in mutants for the transcriptional repressor *Drap1* (Iratni et al., 2002), or combined inactivation of the Nodal antagonists *Lefty1* and *Cerl* (Perea-Gomez et al., 2002).

In the simplest case, Gdf3 may upregulate Nodal pathway activity by signaling in parallel to Nodal itself. However, we cannot exclude the possibility that Gdf3 might create a novel enhanced or diminished activity through heterodimerization with Nodal. The possibility of such heterodimerization with Nodal has been

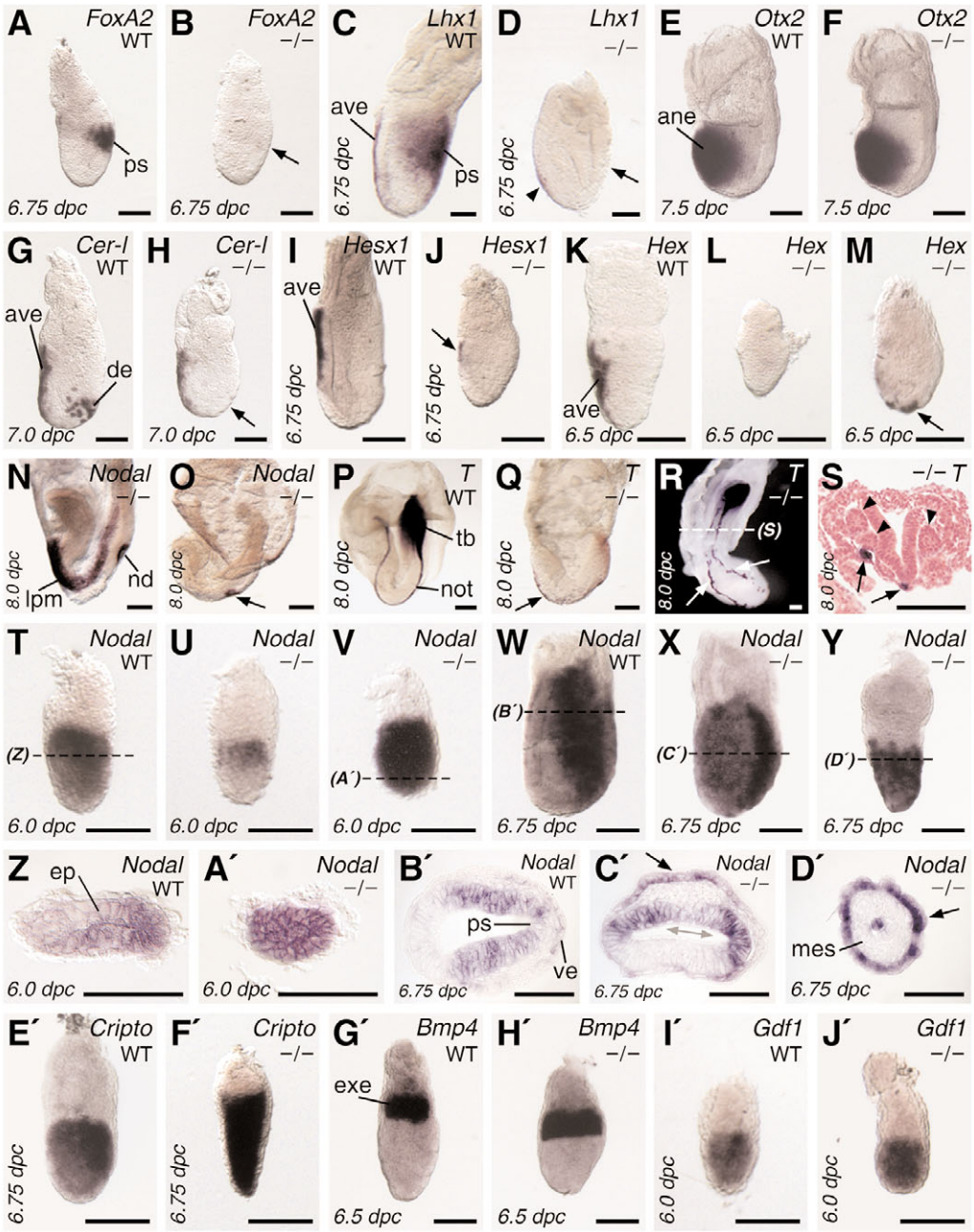

Fig. 6. Phenotypic defects and abnormal *Nodal* expression in *Gdf3* mutants. (**A**,**B**) *Foxa2* is normally expressed in the anterior primitive streak (ps) (A), but is often absent or greatly reduced in *Gdf3* homozygotes (B, arrow). (**C**,**D**) *Lhx1* is expressed in the primitive streak, nascent mesoderm and anterior visceral endoderm (ave) (C), but is frequently absent (D, arrow) or greatly reduced (D, arrowhead) in *Gdf3* mutants. (**E**,**F**) Expression of *Otx2* in the anterior neuroectoderm (ane) is unaffected in *Gdf3* homozygotes. (**G**,**H**) Expression of *Cerl* marks the AVE and definitive endoderm (de), but the definitive endoderm is often absent in *Gdf3* homozygotes (H, arrow). (**I**,**J**) *Hesx1* expression in the AVE is sometimes reduced or absent in *Gdf3*$^{-/-}$ embryos (J, arrow). (**K**-**M**) *Hex* expression in the AVE is sometimes completely absent (L) or is misplaced distally (M, arrow). (**N**,**O**) Asymmetric expression of *Nodal* in the left lateral plate mesoderm (lpm) is observed in *Gdf3*$^{-/-}$ embryos with normal morphology at 8.0 dpc (N); a few abnormal mutants lack *Nodal* expression in the lateral plate, but retain expression around the node (nd) (O, arrow). (**P**,**Q**) Expression of *T* (brachyury) marks the tailbud (tb) and notochord (not) at 8.0 dpc (P), but is absent or greatly reduced in abnormal *Gdf3*$^{-/-}$ embryos (Q, arrow). (**R**,**S**) In rare *Gdf3* homozygotes, expression of *T* reveals a partial axis duplication (R, arrows), corresponding to formation of twinned notochords (S, arrows) and multiple somites (arrowheads). (**T**-**D′**) Expression of *Nodal* is found in the proximal-posterior epiblast (ep) at 6.0 dpc (T,Z), but is downregulated in some *Gdf3* mutants (U) while upregulated in others (V,A′). At 6.75 dpc, *Nodal* is expressed in the posterior epiblast and in the visceral endoderm (ve) overlying the primitive streak (W,B′), but some *Gdf3*$^{-/-}$ embryos show an expansion of the primitive streak (X,C′, double-headed arrow) that is accompanied by increased expression in the visceral endoderm (C′, arrow). Abnormal *Gdf3*$^{-/-}$ embryos with the 'conical' morphology (Y) show high-level *Nodal* expression circumferentially in the visceral endoderm surrounding a thick mesodermal layer (mes) (D′, arrow). (**E′**,**F′**) Expression of *Cripto* in the proximal-posterior epiblast at 6.75 dpc is unaffected in most *Gdf3* homozygotes, but is upregulated in 'conical' mutants (F′). (**G′**,**H′**) *Bmp4* expression in the extra-embryonic ectoderm (exe) at 6.5 dpc is unaffected in *Gdf3* mutants. (**I′**,**J′**) Expression of *Gdf1* in the pre-gastrulation epiblast is unaffected in *Gdf3* homozygotes. Scale bars: 100 μm for A-Y,E′-J′; 50 μm for Z-D′.

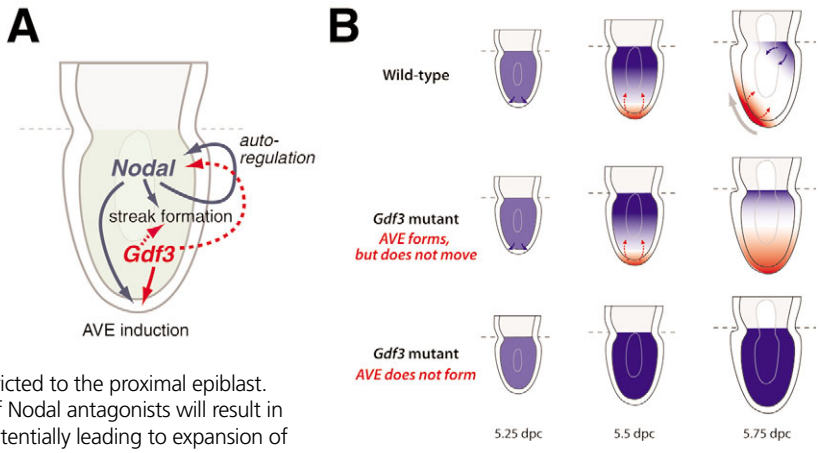

Fig. 7. Model for *Gdf3* function. (**A**) In wild-type embryos, *Nodal* activity promotes AVE induction and movement as well as primitive streak formation, and maintains its expression through an autoregulatory feedback loop. *Gdf3* is also required for AVE formation and movement, and may additionally be necessary for streak formation and maintenance of *Nodal* expression. (**B**) In wild-type embryos (top), expression of Nodal antagonists by the AVE provides essential signals for patterning of the anterior epiblast; the distribution of Nodal pathway activity (including Gdf3) in the epiblast is depicted in blue, while that of Nodal antagonists is shown in red. In the absence of *Gdf3*, the AVE may form but be unable to move (middle), thereby resulting in embryos with downregulated *Nodal* expression that is restricted to the proximal epiblast. Alternatively, if the AVE fails to form (bottom), the absence of Nodal antagonists will result in upregulation of *Nodal* expression throughout the epiblast, potentially leading to expansion of the primitive streak and axis duplication.

demonstrated in principle for Bmp7 (Yeo and Whitman, 2001), as well as for the *Xenopus* Tgfβ factor Derriere (Eimon and Harland, 2002). Whether such heterodimerization is physiologically relevant remains to be elucidated.

Potential overlapping activities of Nodal pathway ligands in early embryogenesis

Our functional analysis of *Gdf3* suggests that the activities of *Vg1*-related genes at pre-gastrulation stages are conserved in vertebrate embryos. In particular, chick *Vg1* is expressed at early pre-streak stages in the epiblast of the posterior marginal zone from stage X to XII (Shah et al., 1997), and has been proposed to cooperate with Wnt and FGF signals in primitive streak formation and initiation of *Nodal* expression (Bertocchini et al., 2004; Skromne and Stern, 2001). Similarly, *Xenopus Vg1* transcripts are localized to vegetal cells at the blastula stage, and have been suggested to play a central role in dorsal mesoderm and endoderm formation (Joseph and Melton, 1998; Kessler and Melton, 1995; Thomsen and Melton, 1993; Weeks and Melton, 1987). These putative functions of *Vg1*-related genes are generally consistent with our findings that mouse *Gdf3* mutants display defects in formation of the AVE, mesoderm and definitive endoderm.

Interestingly, the conserved functions of *Xenopus Vg1* may have been divided between *Gdf1* and *Gdf3,* its mammalian counterparts. The patterns of *Gdf1* and *Gdf3* expression in the epiblast are strikingly complementary, with *Gdf3* being downregulated shortly after 6.0 dpc and *Gdf1* being upregulated at ~5.75 dpc, when it can be detected throughout the epiblast (Wall et al., 2000) (this work). Null mutants for *Gdf1* are defective for left-right axis specification (Rankin et al., 2000), consistent with the proposed role for *Vg1* in coordinating left-right patterning in *Xenopus* (Hyatt et al., 1996; Hyatt and Yost, 1998; Kramer and Yost, 2002). Notably, the phenotype of *Gdf1* mutants is indistinguishable from that of *Cryptic* mutants (Yan et al., 1999), suggesting that Gdf1 signaling may be facilitated by Cryptic in vivo.

The potential overlapping functions of Nodal, Gdf3 and Gdf1 suggests that the Nodal signaling pathway may play as yet poorly understood roles in pre-implantation and early post-implantation development. This possibility is supported by the expression patterns of *Gdf3* and *Nodal* in pre-gastrulation embryos, as well as by the conserved expression of *Nodal, Cripto, Lefty1* and *Gdf3* in undifferentiated mouse and human ES cells (Besser, 2004; Bhattacharya et al., 2004; Ramalho-Santos et al., 2002; Sato et al., 2003). Moreover, recent studies have also suggested a role for Nodal signaling in maintaining the undifferentiated state of human ES cells (James et al., 2005; Vallier et al., 2004). These observations lead us to speculate that this pathway may play a broader role in mammalian embryogenesis than previously conceived.

We would like to thank Brigid Hogan for sharing unpublished information, Se-Jin Lee and Malcolm Whitman for plasmid reagents, Pei Wang, Lei Chen and Hua Chang for expert technical assistance, Marianna de Julio for advice on real-time PCR analysis, and Cory Abate-Shen and Rick Padgett for discussion and comments on the manuscript. This work was supported by grants from the American Heart Association (R.H.), March of Dimes (R.H.) and the National Institutes of Health (HL67355 and HD41648 to S.M.W., HD32067 to M.M.M., HD42837 to M.M.S., and HD01156 and HD27823 to C.W.B.), and by the Robert Wood Johnson Foundation. C.W.B. was a recipient of a Burroughs Wellcome Fund Career Award in the Biomedical Sciences.

Supplementary material

Supplementary material for this article is available at
http://dev.biologists.org/cgi/content/full/133/2/319/DC1

References

Bertocchini, F. and Stern, C. D. (2002). The hypoblast of the chick embryo positions the primitive streak by antagonizing nodal signaling. *Dev. Cell* **3**, 735-744.

Bertocchini, F., Skromne, I., Wolpert, L. and Stern, C. D. (2004). Determination of embryonic polarity in a regulative system: evidence for endogenous inhibitors acting sequentially during primitive streak formation in the chick embryo. *Development* **131**, 3381-3390.

Besser, D. (2004). Expression of nodal, lefty-a, and lefty-B in undifferentiated human embryonic stem cells requires activation of Smad2/3. *J. Biol. Chem.* **279**, 45076-45084.

Bhattacharya, B., Miura, T., Brandenberger, R., Mejido, J., Luo, Y., Yang, A. X., Joshi, B. H., Ginis, I., Thies, R. S., Amit, M. et al. (2004). Gene expression in human embryonic stem cell lines: unique molecular signature. *Blood* **103**, 2956-2964.

Bradley, A. (1987). Production and analysis of chimeric mice. In *Teratocarcinomas and Embryonic Stem Cells: A Practical Approach* (ed. E. J. Robinson), pp. 113-151. Oxford: IRL Press.

Brennan, J., Lu, C. C., Norris, D. P., Rodriguez, T. A., Beddington, R. S. and Robertson, E. J. (2001). Nodal signalling in the epiblast patterns the early mouse embryo. *Nature* **411**, 965-969.

Burt, D. W. and Law, A. S. (1994). Evolution of the transforming growth factor-beta superfamily. *Prog. Growth Factor Res.* **5**, 99-118.

Chang, H., Brown, C. W. and Matzuk, M. M. (2002). Genetic analysis of the mammalian transforming growth factor-beta superfamily. *Endocr. Rev.* **23**, 787-823.

Chen, C. and Shen, M. M. (2004). Two modes by which Lefty proteins inhibit Nodal signaling. *Curr. Biol.* **14**, 618-624.

Cheng, S. K., Olale, F., Bennett, J. T., Brivanlou, A. H. and Schier, A. F. (2003). EGF-CFC proteins are essential coreceptors for the TGF-beta signals Vg1 and GDF1. *Genes Dev.* **17**, 31-36.

Cheng, S. K., Olale, F., Brivanlou, A. H. and Schier, A. F. (2004). Lefty blocks a subset of TGFbeta signals by antagonizing EGF-CFC coreceptors. *PLoS Biol.* **2**, E30.

Conlon, F. L., Lyons, K. M., Takaesu, N., Barth, K. S., Kispert, A., Herrmann,

B. and Robertson, E. J. (1994). A primary requirement for nodal in the formation and maintenance of the primitive streak in the mouse. *Development* **120**, 1919-1928.
Ding, J., Yang, L., Yan, Y. T., Chen, A., Desai, N., Wynshaw-Boris, A. and Shen, M. M. (1998). *Cripto* is required for correct orientation of the anterior-posterior axis in the mouse embryo. *Nature* **395**, 702-707.
Dohrmann, C. E., Kessler, D. S. and Melton, D. A. (1996). Induction of axial mesoderm by zDVR-1, the zebrafish orthologue of Xenopus Vg1. *Dev. Biol.* **175**, 108-117.
Dunn, N. R., Vincent, S. D., Oxburgh, L., Robertson, E. J. and Bikoff, E. K. (2004). Combinatorial activities of Smad2 and Smad3 regulate mesoderm formation and patterning in the mouse embryo. *Development* **131**, 1717-1728.
Eimon, P. M. and Harland, R. M. (2002). Effects of heterodimerization and proteolytic processing on Derriere and Nodal activity: implications for mesoderm induction in Xenopus. *Development* **129**, 3089-3103.
Graff, J. M., Bansal, A. and Melton, D. A. (1996). Xenopus Mad proteins transduce distinct subsets of signals for the TGF beta superfamily. *Cell* **85**, 479-487.
Gritsman, K., Zhang, J., Cheng, S., Heckscher, E., Talbot, W. S. and Schier, A. F. (1999). The EGF-CFC protein one-eyed pinhead is essential for nodal signaling. *Cell* **97**, 121-132.
Habas, R., Kato, Y. and He, X. (2001). Wnt/Frizzled activation of Rho regulates vertebrate gastrulation and requires a novel Formin homology protein Daam1. *Cell* **107**, 843-854.
Helde, K. A. and Grunwald, D. J. (1993). The DVR-1 (Vg1) transcript of zebrafish is maternally supplied and distributed throughout the embryo. *Dev. Biol.* **159**, 418-426.
Hoodless, P. A., Tsukazaki, T., Nishimatsu, S., Attisano, L., Wrana, J. L. and Thomsen, G. H. (1999). Dominant-negative Smad2 mutants inhibit activin/Vg1 signaling and disrupt axis formation in Xenopus. *Dev. Biol.* **207**, 364-379.
Hoodless, P. A., Pye, M., Chazaud, C., Labbe, E., Attisano, L., Rossant, J. and Wrana, J. L. (2001). FoxH1 (Fast) functions to specify the anterior primitive streak in the mouse. *Genes Dev.* **15**, 1257-1271.
Hyatt, B. A. and Yost, H. J. (1998). The left-right coordinator: the role of Vg1 in organizing left-right axis formation. *Cell* **93**, 37-46.
Hyatt, B. A., Lohr, J. L. and Yost, H. J. (1996). Initiation of vertebrate left-right axis formation by maternal Vg1. *Nature* **384**, 62-65.
Iratni, R., Yan, Y. T., Chen, C., Ding, J., Zhang, Y., Price, S. M., Reinberg, D. and Shen, M. M. (2002). Inhibition of excess nodal signaling during mouse gastrulation by the transcriptional corepressor DRAP1. *Science* **298**, 1996-1999.
James, D., Levine, A. J., Besser, D. and Hemmati-Brivanlou, A. (2005). TGF{beta}/activin/nodal signaling is necessary for the maintenance of pluripotency in human embryonic stem cells. *Development* **132**, 1273-1282.
Jones, C. M., Simon-Chazottes, D., Guenet, J. L. and Hogan, B. L. (1992). Isolation of Vgr-2, a novel member of the transforming growth factor-beta-related gene family. *Mol. Endocrinol.* **6**, 1961-1968.
Jones, C. M., Kuehn, M. R., Hogan, B. L., Smith, J. C. and Wright, C. V. (1995). Nodal-related signals induce axial mesoderm and dorsalize mesoderm during gastrulation. *Development* **121**, 3651-3662.
Joseph, E. M. and Melton, D. A. (1997). Xnr4: a Xenopus nodal-related gene expressed in the Spemann organizer. *Dev. Biol.* **184**, 367-372.
Joseph, E. M. and Melton, D. A. (1998). Mutant Vg1 ligands disrupt endoderm and mesoderm formation in Xenopus embryos. *Development* **125**, 2677-2685.
Kato, Y., Habas, R., Katsuyama, Y., Naar, A. M. and He, X. (2002). A component of the ARC/Mediator complex required for TGF beta/Nodal signalling. *Nature* **418**, 641-646.
Kessler, D. S. and Melton, D. A. (1995). Induction of dorsal mesoderm by soluble, mature Vg1 protein. *Development* **121**, 2155-2164.
Kramer, K. L. and Yost, H. J. (2002). Ectodermal syndecan-2 mediates left-right axis formation in migrating mesoderm as a cell-nonautonomous Vg1 cofactor. *Dev. Cell* **2**, 115-124.
Lowe, L. A., Yamada, S. and Kuehn, M. R. (2001). Genetic dissection of nodal function in patterning the mouse embryo. *Development* **128**, 1831-1843.
Lu, C. C., Brennan, J. and Robertson, E. J. (2001). From fertilization to gastrulation: axis formation in the mouse embryo. *Curr. Opin. Genet. Dev.* **11**, 384-392.
Matzuk, M. M., Finegold, M. J., Su, J. G., Hsueh, A. J. and Bradley, A. (1992). Alpha-inhibin is a tumour-suppressor gene with gonadal specificity in mice. *Nature* **360**, 313-319.
McPherron, A. C. and Lee, S. J. (1993). GDF-3 and GDF-9: two new members of the transforming growth factor-beta superfamily containing a novel pattern of cysteines. *J. Biol. Chem.* **268**, 3444-3449.
Melton, D. A. (1987). Translocation of a localized maternal mRNA to the vegetal pole of Xenopus oocytes. *Nature* **328**, 80-82.
Newfeld, S. J., Wisotzkey, R. G. and Kumar, S. (1999). Molecular evolution of a developmental pathway: phylogenetic analyses of transforming growth factor-beta family ligands, receptors and Smad signal transducers. *Genetics* **152**, 783-795.
Norris, D. P., Brennan, J., Bikoff, E. K. and Robertson, E. J. (2002). The FoxH1-dependent autoregulatory enhancer controls the level of Nodal signals in the mouse embryo. *Development* **129**, 3455-3468.
Perea-Gomez, A., Vella, F. D., Shawlot, W., Oulad-Abdelghani, M., Chazaud, C., Meno, C., Pfister, V., Chen, L., Robertson, E., Hamada, H. et al. (2002). Nodal antagonists in the anterior visceral endoderm prevent the formation of multiple primitive streaks. *Dev. Cell* **3**, 745-756.
Ramalho-Santos, M., Yoon, S., Matsuzaki, Y., Mulligan, R. C. and Melton, D. A. (2002). "Stemness": transcriptional profiling of embryonic and adult stem cells. *Science* **298**, 597-600.
Rankin, C. T., Bunton, T., Lawler, A. M. and Lee, S. J. (2000). Regulation of left-right patterning in mice by growth/differentiation factor-1. *Nat. Genet.* **24**, 262-265.
Reissmann, E., Jornvall, H., Blokzijl, A., Andersson, O., Chang, C., Minchiotti, G., Persico, M. G., Ibanez, C. F. and Brivanlou, A. H. (2001). The orphan receptor ALK7 and the Activin receptor ALK4 mediate signaling by Nodal proteins during vertebrate development. *Genes Dev.* **15**, 2010-2022.
Rivera-Perez, J. A., Mager, J. and Magnuson, T. (2003). Dynamic morphogenetic events characterize the mouse visceral endoderm. *Dev. Biol.* **261**, 470-487.
Rossant, J. and Tam, P. P. (2004). Emerging asymmetry and embryonic patterning in early mouse development. *Dev. Cell* **7**, 155-164.
Saijoh, Y., Oki, S., Tanaka, C., Nakamura, T., Adachi, H., Yan, Y. T., Shen, M. M. and Hamada, H. (2005). Two nodal-responsive enhancers control. left-right asymmetric expression of Nodal. *Dev. Dyn.* **232**, 1031-1036.
Sato, N., Sanjuan, I. M., Heke, M., Uchida, M., Naef, F. and Brivanlou, A. H. (2003). Molecular signature of human embryonic stem cells and its comparison with the mouse. *Dev. Biol.* **260**, 404-413.
Schier, A. F. (2003). Nodal signaling in vertebrate development. *Annu. Rev. Cell Dev. Biol.* **19**, 589-621.
Schier, A. F. and Shen, M. M. (2000). Nodal signalling in vertebrate development. *Nature* **403**, 385-389.
Seleiro, E. A., Connolly, D. J. and Cooke, J. (1996). Early developmental expression and experimental axis determination by the chicken Vg1 gene. *Curr. Biol.* **6**, 1476-1486.
Shah, S. B., Skromne, I., Hume, C. R., Kessler, D. S., Lee, K. J., Stern, C. D. and Dodd, J. (1997). Misexpression of chick Vg1 in the marginal zone induces primitive streak formation. *Development* **124**, 5127-5138.
Skromne, I. and Stern, C. D. (2001). Interactions between Wnt and Vg1 signalling pathways initiate primitive streak formation in the chick embryo. *Development* **128**, 2915-2927.
Song, J., Oh, S. P., Schrewe, H., Nomura, M., Lei, H., Okano, M., Gridley, T. and Li, E. (1999). The type II activin receptors are essential for egg cylinder growth, gastrulation, and rostral head development in mice. *Dev. Biol.* **213**, 157-169.
Srinivas, S., Rodriguez, T., Clements, M., Smith, J. C. and Beddington, R. S. (2004). Active cell migration drives the unilateral movements of the anterior visceral endoderm. *Development* **131**, 1157-1164.
Takahashi, S., Yokota, C., Takano, K., Tanegashima, K., Onuma, Y., Goto, J. and Asashima, M. (2000). Two novel nodal-related genes initiate early inductive events in Xenopus Nieuwkoop center. *Development* **127**, 5319-5329.
Thomas, P. Q., Brown, A. and Beddington, R. S. P. (1998). *Hex*: a homeobox gene revealing peri-implantation asymmetry in the mouse embryo and an early transient marker of endothelial cell precursors. *Development* **125**, 85-94.
Thomsen, G. H. and Melton, D. A. (1993). Processed Vg1 protein is an axial mesoderm inducer in Xenopus. *Cell* **74**, 433-441.
Vallier, L., Reynolds, D. and Pedersen, R. A. (2004). Nodal inhibits differentiation of human embryonic stem cells along the neuroectodermal default pathway. *Dev. Biol.* **275**, 403-421.
Vincent, S. D., Dunn, N. R., Hayashi, S., Norris, D. P. and Robertson, E. J. (2003). Cell fate decisions within the mouse organizer are governed by graded Nodal signals. *Genes Dev.* **17**, 1646-1662.
Waldrip, W. R., Bikoff, E. K., Hoodless, P. A., Wrana, J. L. and Robertson, E. J. (1998). Smad2 signaling in extraembryonic tissues determines anterior-posterior polarity of the early mouse embryo. *Cell* **92**, 797-808.
Wall, N. A., Craig, E. J., Labosky, P. A. and Kessler, D. S. (2000). Mesendoderm induction and reversal of left-right pattern by mouse Gdf1, a Vg1-related gene. *Dev. Biol.* **227**, 495-509.
Watanabe, M. and Whitman, M. (1999). FAST-1 is a key maternal effector of mesoderm inducers in the early Xenopus embryo. *Development* **126**, 5621-5634.
Weeks, D. L. and Melton, D. A. (1987). A maternal mRNA localized to the vegetal hemisphere in Xenopus eggs codes for a growth factor related to TGF-beta. *Cell* **51**, 861-867.
Whitman, M. (2001). Nodal signaling in early vertebrate embryos. Themes and variations. *Dev. Cell* **1**, 605-617.
Wilkinson, D. G. (1992). *In Situ Hybridization: A Practical Approach*. London: Oxford University Press.
Yamamoto, M., Meno, C., Sakai, Y., Shiratori, H., Mochida, K., Ikawa, Y., Saijoh, Y. and Hamada, H. (2001). The transcription factor FoxH1 (FAST) mediates Nodal signaling during anterior-posterior patterning and node formation in the mouse. *Genes Dev.* **15**, 1242-1256.

Yamamoto, M., Saijoh, Y., Perea-Gomez, A., Shawlot, W., Behringer, R. R., Ang, S. L., Hamada, H. and Meno, C. (2004). Nodal antagonists regulate formation of the anteroposterior axis of the mouse embryo. *Nature* **428**, 387-392.

Yan, Y.-T., Gritsman, K., Ding, J., Burdine, R. D., Corrales, J. D., Price, S. M., Talbot, W. S., Schier, A. F. and Shen, M. M. (1999). Conserved requirement for *EGF-CFC* genes in vertebrate left-right axis formation. *Genes Dev.* **13**, 2527-2537.

Yan, Y. T., Liu, J. J., Luo, Y., Chaosu, E., Haltiwanger, R. S., Abate-Shen, C. and Shen, M. M. (2002). Dual roles of Cripto as a ligand and coreceptor in the Nodal signaling pathway. *Mol. Cell. Biol.* **22**, 4439-4449.

Yeo, C. and Whitman, M. (2001). Nodal signals to Smads through Cripto-dependent and Cripto-independent mechanisms. *Mol. Cell* **7**, 949-957.

Zhou, X., Sasaki, H., Lowe, L., Hogan, B. L. and Kuehn, M. R. (1993). Nodal is a novel TGF-beta-like gene expressed in the mouse node during gastrulation. *Nature* **361**, 543-547.